JOURNAL OF SOLID STATE CHEMISTRY 97, 319–331 (1992)

The Molecular Structure of Bismuth Oxide by Raman Spectroscopy

FRANKLIN D. HARDCASTLE* AND ISRAEL E. WACHS

Departments of Chemistry and Chemical Engineering, Zettlemoyer Center for Surface Studies, Lehigh University, Bethlehem, Pennsylvania 18015

Received May 23, 1990; in revised form June 3, 1991

A new method is presented for interpreting the Raman spectra of bismuth oxides. The method relies on empirical relations between bismuth–oxygen (Bi–O) bond lengths, bond strengths, and Raman stretching frequencies. A least-squares exponential fit of crystallographically determined Bi–O bond lengths and Raman stretching frequencies is presented along with a relation between Bi–O bond strengths, in valence units, and Raman stretching frequencies. The empirical bond length/bond strength/Raman stretching frequency relationships lead to a unique and effective method of interpreting Raman spectra of bismuth oxide species. This method allows the systematic determination of the Bi–O bond lengths and oxygen coordination of a BiO_x polyhedron from its Raman spectrum. The utility of the method is illustrated by estimating the Raman stretching frequencies for ideally symmetric bismuth oxide structures BiO_4, BiO_5, BiO_6, BiO_7, and BiO_8. As a final, practical example the method is used to determine the bond lengths and coordinations of the bismuth oxide species in the β- and δ-phases of Bi_2O_3. This new approach for evaluating the Raman spectra of bismuth oxide species is expected to be generally applicable to all bismuth oxides, regardless of environment, physical state, or oxidation state.

I. Introduction

The four known polymorphs of bismuth oxide, labeled as α-, β-, δ-, and γ-Bi_2O_3, have been extensively studied because of their interesting physical properties (*1–8*). In particular, the β-, δ-, and γ-phases exhibit ionic conductivity with δ-Bi_2O_3 being one of the best ionic conductors known (*2*); the oxide ions in δ-Bi_2O_3 are thought to be the mobile charge carriers. The γ-phase of Bi_2O_3, having the sillenite structure, is optically active and shows promise as an electrooptic device (*9–11*). Some of the ternary oxides derived from bismuth oxide—for example, Bi_2O_3–Nb_2O_5, Bi_2O_3–MoO_3, Bi_2O_3–WO_3, and Bi_2O_3–V_2O_5—are catalytically active for selective oxidation and ammoxidation reactions (*5*). In fact, many of these catalytically active systems contain bismuth-rich phases, and the possible catalytic role played by the bismuth phases is under investigation (*3, 4*).

The polymorphism of the bismuth oxide system has also been studied with the aim of relating its unusual physical properties with molecular structure (*12–16*). The monoclinic phase, α-Bi_2O_3, undergoes a phase transformation at 729°C to cubic δ-Bi_2O_3. Upon cooling, δ-Bi_2O_3 may transform to either tetragonal β-Bi_2O_3, at 650°C, or body-centered cubic γ-Bi_2O_3, at 639°C. Both the β- and δ-phases of Bi_2O_3 are metastable and exist as pure phases only at elevated temperatures, but may be stabilized to room tem-

*Present address: Division 1845, Sandia National Laboratories, Albuquerque, NM 87185.

0022-4596/92 $3.00

perature by the addition of metal cation impurities such as niobium or tantalum. Although the molecular structures of the bismuth oxide polyhedra have been determined for the well-ordered α- and γ-phases of Bi_2O_3, the structures of the bismuth oxide species in the metastable β- and δ-phases have not been reported.

Raman spectroscopy promises to offer insight into the structures of bismuth oxide molecular species because, in general, the Raman bands reflect the bond lengths, bond strengths, and overall symmetry of metal oxide species. This is not only true for the more common crystalline and solution phases (*17*), but also for the exotic two-dimensional surface phases (*18, 19*). The basic idea behind the Raman analysis is that different molecular structures typically have different types of bonds, and this, in turn, leads to a different set of Raman spectral features. Used in this way, Raman spectroscopy is an effective structural tool because it can be used to discriminate or "fingerprint" between alternate structures proposed for a chemical species.

Recently, a new, systematic approach (*20*) has been developed for interpreting the Raman spectra of transition metal oxides. This approach regards each metal–oxygen bond in a molecular species or crystalline lattice as vibrationally independent of its surroundings so that a direct relationship may be formulated between its metal–oxygen Raman stretching frequencies and bond lengths. Naturally, this approach does not lead to a vibrational mode analysis because it neglects nearest-neighbor interactions and, consequently, bending/wagging and external modes. Furthermore, this approach fails to distinguish between symmetric and antisymmetric stretching modes. Within the limits of experimental error afforded by crystallographic bond length determinations, however, this approach is justified and may be used to determine metal–oxygen bond lengths from Raman stretching frequencies because the effect of the interaction force constants on the bond lengths is smaller than the uncertainty associated with most crystallographic bond length determinations. Applying this reasoning, empirical relations have already been established for relating molybdenum- (*21*), vanadium- (*22*), niobium- (*23*), tungsten- (*24*), and titanium–oxygen (*25*) bond lengths to their observed Raman stretching frequencies for reference compounds.

In the present study, an empirical, exponential relationship is noted between bismuth–oxygen (Bi–O) bond lengths and their respective Raman stretching frequencies. The combined use of the Raman stretching frequency/bond length and bond length/bond strength empirical relations leads to an effective and simple method of determining the Bi–O bond lengths and coordinations of bismuth oxide molecular species. This approach is used to estimate Raman stretching frequencies for ideal bismuth oxide structures and to propose molecular structures for the bismuth oxide species in the β- and δ-phases of Bi_2O_3.

II. Experimental

The impurity-stabilized β-, δ-, and γ-phases of Bi_2O_3 were kindly provided by D. A. Jefferson, W. Zhou, and J. M. Thomas. In their preparations, β-Bi_2O_3 was stabilized to room temperature by mixing α-Bi_2O_3 with Nb_2O_5 (both of 99.9% purity) at a ratio of Bi : Nb = 60 : 1, grinding a slurry of the weighed mixture with acetone followed by drying in air, and heating in oxygen at 820°C for 113 hr (*26*). δ-Bi_2O_3 was stabilized in a similar manner by mixing α-Bi_2O_3 with Nb_2O_5 or Ta_2O_5 at a ratio of Bi : M = 4 : 1 and heating to 820°C for 116 hr (*27*). These samples have been previously characterized by X-ray powder diffraction, electron diffraction, and high-resolution electron microscopy (*26–28*).

The Raman spectra were collected by us-

ing 10–40 mW of the 514.5-nm line of a Spectra-Physics argon ion laser (Model 171) for excitation. The laser beam power was measured at the sample. The diffusely scattered radiation from the sample was collected in a 90° scattering geometry and directed into a Spex Triplemate spectrometer (Model 1877) coupled to an intensified photodiode array detector (880 intensified array elements) and optical multichannel analyzer (OMA III, Princeton Applied Research, Model 1463). The detector was thermoelectrically cooled to −35°C. The Raman spectra were collected and recorded with an OMA III (PAR) dedicated computer and software. The spectral resolution and reproducibility were experimentally determined to be better than 2 cm^{-1}.

The Raman spectra of the following bismuth oxide compounds were collected: α-Bi_2O_3, β-Bi_2O_3 (Bi : Nb = 60 : 1), δ-Bi_2O_3 (Bi : Ta = 4 : 1, Bi : Nb = 4 : 1), γ-Bi_2O_3 (Bi : V = 60 : 1), and $BaBiO_3$. About 100–200 mg of each bismuth oxide sample was pressed into a thin water of about 1-mm thickness with a KBr backing for mechanical support. Each pressed sample was mounted onto a sample holder (Spex, Model 1445A) capable of rotating at about 200 rpm to avoid local heating effects caused by the focused laser beam. The Raman spectra of the reference compounds $Bi_{12}GeO_{20}$, $Bi_{12}SiO_{20}$, $Bi_{12}TiO_{20}$, and $Bi_{38}ZnO_{60}$ were taken from the literature.

III. Theory

The interpretation of the Raman spectrum of a transition metal oxide species in the solid state is facilitated by imposing two levels of approximation. First, the internal and external modes of the crystal are assumed to be independent of one another. The internal modes of metal oxide molecules within the unit cell of a crystal occur in the medium- and high-frequency regions (>200 cm^{-1} for bismuth oxide) while the external modes, including translational and librational modes, occur at lower frequencies (<200 cm^{-1}). Second, the site-symmetry approximation (*29*), or correlation method, may be made by assigning a high degree of symmetry to each atom, or site, within the unit cell. Although the site symmetry approach leads to the total number and types of infrared and Raman active modes expected from the crystal, a detailed knowledge of the crystal structure is first required in order to perform the vibrational mode analysis. The site-symmetry approach allows the internal modes of a molecular species confined to a crystalline lattice to be directly compared with those of a similar molecule in solution or the gas phase. Consequently, the site-symmetry approach forms the basis of the fingerprint method of identifying molecular geometries. For metal oxides with distorted molecular geometries, however, the fingerprint approach cannot be reliably used because of inconsistent matches between spectra due to a virtually infinite number of geometric irregularities possible for a distorted metal oxide species. Clearly, there is a demonstrated need for a systematic way of determining molecular structures from Raman spectra that does not rely on the subjectivity and uncertainty involved with fingerprinting characteristic vibrational bands. Furthermore, the desired systematic method would be generally applicable so that it would be capable of yielding detailed structural information not only for ideally symmetric geometries, but also for distorted metal oxide species.

Recently, empirical relations have been found between the metal–oxygen Raman stretching frequencies and metal–oxygen bond lengths for several transition metal oxide systems including molybdenum- (*21*), vanadium- (*22*), niobium- (*23*), tungsten- (*24*), and titanium-oxygen (*25*) bonds. In each case, the empirical Raman stretching frequency/bond length relationship was found to follow a simple exponential form,

$$\nu = A \exp(BR), \quad (1)$$

where A and B are fitting parameters, ν is the Raman stretching frequency in wavenumbers, and R is the metal–oxygen bond length in angstroms. In the present study, Eq. (1) is also found to adequately describe the relation between the Raman stretching frequencies and bond lengths of bismuth–oxygen bonds that are present in bismuth oxide reference compounds.

The Pauling bond strengths, in valence units, also referred to as bond orders or bond valences, of metal–oxygen bonds are useful for discussing the plausibility of proposed metal oxide structures (*30*). The Pauling bond strength of a bond reflects the relative distribution of available valence electrons throughout the covalent bonds of a metal oxide species. Furthermore, according to the valence sum rule, there is a conservation of valency associated with the metal cation, and this allows the valence sum rule to serve as a bookkeeping device for the number of valence electrons in that structure. Hence, the calculated valence state of a proposed structure may be compared to the formal oxidation state of the metal cation as a simple test for the plausibility of the structure.

Brown and Wu (*31*) developed a generally applicable relationship that relates the metal–oxygen bond valence s to its interatomic distance R. Specifically, the empirical expression relating a Bi–O bond length, in angstroms, to its bond strength in valence units is

$$s(\text{Bi–O}) = (R/2.010)^{-5.0}, \quad (2)$$

where 2.010 Å is the estimated bond length of a Bi–O bond of unit valency. The empirical parameters in Eq. (2), 2.010 and 5.0, were determined from the data of seven different Bi^{3+} cation environments.

IV. Results

The bismuth–oxygen bond lengths, obtained from the reported values of several bismuth oxide compounds, were assigned to their respective Raman stretching frequencies. The bismuth oxide reference compounds are listed in Table I, where their reported Bi–O bond lengths, assigned Raman stretching frequencies, calculated bond strengths (from Eq. (2)), and bismuth cation valence states (by the valence sum rule) are tabulated.

The assignment of the Raman bands to Bi–O bond lengths is straightforward for several of the reference compounds. Huber and Herzberg (*32*) have tabulated five different bond lengths and fundamental stretching frequencies for the diatomic BiO molecule and all are included in Table I. The double perovskite $BaBiO_3$, more accurately expressed as $Ba_2Bi^{3+}Bi^{5+}O_6$, exhibits only two Raman bands at 568 and 308 cm^{-1}, and these are assigned to the two average bond lengths of 2.12 and 2.28 Å, respectively, reported for the $Bi^{5+}O_6$ and $Bi^{3+}O_6$ octahedra present in the $BaBiO_3$ structure (*33*). The sillenite structure of composition $Bi_{25}VO_{40}$ contains nearly perfect $V^{5+}O_4$ tetrahedra where the V–O bond lengths are 1.719(19) Å (*34*); but when the vanadium content is less, as for example in Bi : V = 60 : 1, listed in Table I, Bi^{5+} cations occupy the remainder of the tetrahedral sites and the Raman stretching frequency of this tetrahedron is observed at 827 cm^{-1}. Accordingly, the first entry in Table I includes this $Bi^{5+}O_4$ tetrahedron with estimated Bi–O bond lengths of 1.922 Å (calculated from Eq. (2)) and an observed Raman stretching frequency at 827 cm^{-1}.

The composition of the Bi–Zn–O sillenite structure used by Betsch and White (*35*) in their Raman experiments is the same as or similar to that reported by Craig and Stephenson (*36*) in their single crystal X-ray diffraction study. The Bi–Zn–O sillenite structure was found to have only a narrow compositional range corresponding to the stoichiometric formula $Bi_{38}ZnO_{60}$. Although Betsch and White reported the stoichiomet-

TABLE I

BISMUTH OXIDE REFERENCE COMPOUNDS

Compound	R (Å)	ν (cm^{-1})	s (v.u.)[b]	Valence (v.u.)	Reference
Bi : V = 60 : 1	1.922(4×)	827	1.25	5.0	*20, 34*
BiO (diatomic)	1.934	692	1.21	1.21	*32*
$Bi_{12}GeO_{20}$	2.053	537	0.90		*42*[c]
	2.212	323	0.62		
	2.217	323	0.61		
	2.619	129	0.27		
	2.623	129	0.26		
	3.113		0.11		
	3.200		0.10	2.87	
$Bi_{12}SiO_{20}$	2.056	538	0.89		*42*[c]
	2.203	350	0.63		
	2.209	328	0.62		
	2.642	129	0.25		
	2.657	129	0.25		
	3.076		0.12		
	3.168		0.10	2.87	
$Bi_{38}ZnO_{60}$	2.072	527	0.86		*36*[c]
	2.220	373	0.61		
	2.251	310	0.57		
	2.581	139	0.29		
	2.594	139	0.28		
	3.113		0.11		
	3.206		0.10	2.81	
$Bi_{12}TiO_{20}$	2.075	536	0.85		*44*[c]
	2.222	350	0.61		
	2.241	319	0.58		
	2.603	127	0.27		
	2.606	127	0.27		
	3.094		0.12		
	3.209		0.10	2.80	
BiO (diatomic)	2.09	483	0.82	0.82	*32*
BiO (diatomic)	2.110	465	0.78	0.78	*32*
$BaBiO_3$	2.12(a, 6×)[d]	563	0.71	(a)4.27	*33*
	2.28(b, 6×)	308	0.53	(b)3.19	
α-Bi_2O_3	2.130(a)	446	0.75		*43*[c]
	2.133(b)	446	0.74		
	2.201(a)	338	0.64		
	2.210(b)	314	0.62		
	2.218(b)	314	0.61		
	2.283(a)	282	0.53		
	2.422(a)	210	0.39		
	2.546(b)	158	0.31		
	2.559(a)	151	0.30		
	2.629(b)	139	0.26		
	2.787(a)		0.20		
	3.267(b)		0.09	(a)2.80	
	3.400(b)		0.08	(b)2.70	
BiO (diatomic)	2.142	508	0.73	0.73	*32*
BiO (diatomic)	2.229	343	0.60	0.60	*32*

[a] ν(cm^{-1}): assigned Bi–O Raman stretching frequency.
[b] s (v.u.): Pauling bond strength in valence units (Eq. (2)).
[c] Raman band positions from Ref. (*35*).
[d] (a) and (b) designations represent different bismuth cation sites.

ery of their phase as $Bi_{12}ZnO_{19}$, they used the best Bi : Zn ratio that yielded a single phase material so far as could be determined from X-ray powder diffraction, Raman, and infrared spectroscopic data—this is in agreement with those of both Safronov *et al.* (*37*) and Kargin *et al.* (*38*) at a composition of $Bi_{38}ZnO_{60}$.

The assignment of the Raman stretching frequencies to Bi–O bond lengths for compounds containing networks of interconnecting BiO_x polyhedra is not as straight forward. Three-dimensional networks are expected to exhibit Raman bands in the 200- to 300-cm^{-1} region because of their medium-range order. The Raman bands due to medium-range order are typically sharp and are found at higher frequencies than the lattice vibrations due to long-range order. For example, sharp Raman bands due to medium-range order have been identified in the binary metal oxides V_2O_5 and MoO_3, where three-dimensional networks are present, but not in their corresponding ternary oxides (*21, 22*). Perhaps the most studied example of Raman bands representing medium-range order are the so-called "defect" bands present in the Raman spectrum of vitreous SiO_2. Galeener (*39, 40*) has assigned the extraordinary sharp bands appearing at 606 and 495 cm^{-1} to the presence of three- and four-membered siloxane rings, respectively, in vitreous silica.

The sillenite reference compounds, consisting of $Bi_{12}GeO_{20}$, $Bi_{12}SiO_{20}$, $Bi_{38}ZnO_{60}$, and $Bi_{12}TiO_{20}$, all show a very sharp, intense Raman band due to the medium-range order of the bismuth oxide network in the 251- to 276-cm^{-1} range. The Raman band due to medium-range order in sillenite was visually identified by its sharp spectral characteristic; its assignment was corroborated by showing that this band does not correspond to a Bi–O bond length by using a preliminary exponential fit (Eq. (1)) of the data. Very weak Raman bands at about 620 and 455 cm^{-1} were also not assigned to the stretching of Bi–O bonds; their weak relative intensities indicate that these bands may be due to antisymmetric stretching modes involving two or more neighboring chemical bonds or perhaps to overtones or combination bands (although these effects are quite common in infrared spectroscopy, they are rarely seen in the Raman spectra of transition metal oxides). The Raman bands of the longer Bi–O bonds, of about 2.6 Å, were identified by extrapolating into the low-frequency region. Bi–O bonds of greater than 2.7 Å in length were not assigned to observed Raman bands because of the overwhelming presence of bending/wagging and external modes in the low wavenumber region. Naturally, the Bi–O bond length/stretching frequency relation is not expected to be reliable for determining Bi–O bonds of lengths greater than 2.7 Å because of the unreliability of the band assignments in this region.

The data from Table I consist of 38 points correlating Bi–O Raman stretching frequencies to reported crystallographic bond lengths of bismuth oxide reference compounds. The functional form of this correlation is found to be adequately expressed as a simple exponential function, Eq. (1). The fitting parameters are determined from a nonlinear least-squares treatment of the data. The resulting expression relating Bi–O bond lengths to Raman stretching frequencies is

$$\nu(\mathrm{cm}^{-1}) = 92{,}760 \exp(-2.511R). \quad (3)$$

Equation (3) is plotted in Fig. 1. The standard deviation of estimating a Bi–O bond distance from its Raman stretching frequency by using Eq. (3) is about 0.030 Å. Conversely, the standard deviation of estimating a Raman stretching frequency from an absolute bond length is about 32 cm^{-1}.

Bond valence/stretching frequency correlations are also useful for determining the structures of metal oxide species because the bond valence is representative of the

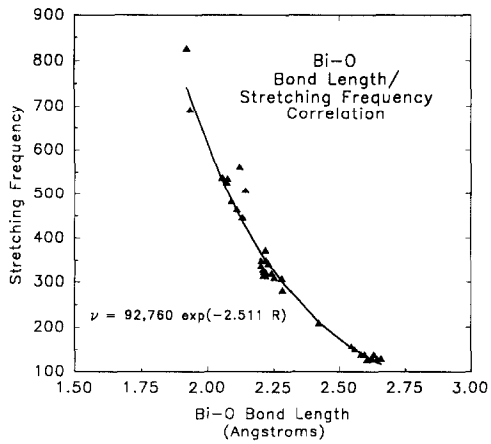

FIG. 1. The empirical correlation between bismuth–oxygen (Bi–O) bond lengths and Raman stretching frequencies, where ν is the frequency in wavenumbers and R is the Bi–O bond length in angstroms.

strength of the chemical bond and denotes the relative number of valence electrons occupying the bond. According to the valence sum rule, the additive contributions of the valences of each of the Bi–O bonds per bismuth cation site should equal the formal oxidation state of the bismuth cation, that is, 3.0 or 5.0 valence units, depending on its oxidation state. The combined use of the empirical bond valence/bond length relation of Brown and Wu, Eq. (2), and the Raman stretching frequency/bond length relation, Eq. (3), yields the following relation between the Pauling Bi–O bond strength s (in valence units) and the Raman stretching frequency:

$$s(\text{Bi–O}) = \{0.198 \ln((92{,}760)/\nu(\text{cm}^{-1}))\}^{-5.0}. \quad (4)$$

Equation (4) is plotted in Fig. 2.

V. Discussion

The general empirical relation between the Raman stretching frequencies of metal–oxygen bonds and their corresponding bond lengths has been previously justified for several transition metal oxide systems (*20–25*). In these previous studies, it was shown that in spite of the vibrational interactions between neighboring metal–oxygen bonds, the net influence of these interaction force constants on the metal–oxygen bond lengths is smaller than the experimental error associated with most bond distance determinations and is determined by the standard deviation of the stretching frequency/bond length correlation (σ = 0.030 Å for Eq. (3)). This means that, to a first approximation, metal–oxygen Raman stretching frequencies may be directly converted to bond lengths and strengths within a specified precision that is limited by the magnitude of vibrational interactions between neighboring chemical bonds. The resulting stretching frequency/bond length/bond strength relationship may be used to deduce possible structures for bismuth oxide species in a systematic way, as illustrated below.

In the following subsections of the Discussion section applications of Eqs. (3) and (4) will be illustrated by estimating Raman stretching frequencies for several ideally

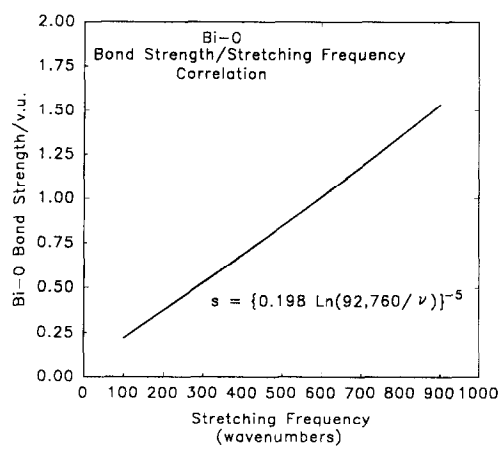

FIG. 2. The empirical correlation between Pauling bond strengths s, in valence units, and Raman stretching frequencies in wavenumbers.

symmetric bismuth oxide structures and by determining the structures of the BiO_x polyhedra present in β- and δ-phases of Bi_2O_3. In order to facilitate in the calculations, a QuickBASIC computer program was written and used to consider all possible combinations of bond strengths consistent with the formal oxidation state of the bismuth cation within a specified tolerance of σ = 0.21 v.u. as determined from the data in Table I. Once the computer program identifies a combination of Bi–O bond strengths consistent with the bismuth oxidation state, the coordination, bond strengths, and bond lengths of the possible bismuth oxide structure are tabulated.

Applications

(1) Estimating stretching frequencies for ideally symmetric bismuth oxide units: BiO_4, BiO_5, BiO_6, BiO_7, and BiO_8. The Raman stretching frequencies of symmetric bismuth oxide species can be easily estimated by using Eqs. (3) and (4). For highly symmetric species, only one type of Bi–O bond is present, one bond length, and therefore only one Raman stretching frequency should be observed in the high-frequency region. For perfectly symmetric structures with more than three atoms, however, both symmetric and antisymmetric stretching frequencies are expected to appear in the Raman spectrum (*41*). Recent work on relating metal–oxygen bond lengths to Raman stretching frequencies has shown that the symmetric and antisymmetric stretching frequencies are close enough in frequency so as to yield the same bond length within the limits of the error associated with the empirical correlations. The reference compounds required to test this hypothesis for the bismuth oxide system, however, are not available; consequently, this hypothesis is cautiously assumed to hold for the bismuth oxide system as well. The hypothesis is based on the assumption that, for a BiO_x polyhedron, the change in Bi–O bond lengths caused by vibrational interactions between Bi–O bonds is less than or comparable to the error associated with crystallographic Bi–O bond length determinations.

TABLE II

ESTIMATED BOND LENGTHS AND RAMAN STRETCHING FREQUENCIES FOR IDEAL BISMUTH OXIDE STRUCTURES

Structure	Bond length (Å)	ν (cm^{-1})	s (v.u.)	Bivalence (v.u.)
BiO_4	1.922	743	1.25	5.00
BiO_4	2.129	442	0.75	3.00
BiO_5	2.010	596	1.00	5.00
BiO_5	2.225	347	0.60	3.01
BiO_6	2.085	493	0.83	5.00
BiO_6	2.309	281	0.50	3.00
BiO_7	2.381	235	0.43	3.00
BiO_8	2.445	200	0.38	3.00

Although Eqs. (3) and (4) may be used to determine bond lengths and strengths from observed Raman bands, it is also possible to derive Raman stretching frequencies from given bond strengths and/or bond lengths. The stretching frequency of an ideal BiO_x unit may be estimated by considering the even distribution of valence throughout the x Bi–O bonds. For example, for a $Bi^{3+}O_6$ octahedron each Bi–O bond has 3.0 v.u. per six Bi–O bonds, or 0.50 v.u. of valence per Bi–O bond. Equation (2) converts this value to a Bi–O bond length of 2.309 Å, and Eq. (3) converts this to a Raman stretching frequency of 281 cm^{-1} for the perfect $Bi^{3+}O_6$ octahedron. Similarly, for a $Bi^{5+}O_6$ octahedron, the 5.0 valence units equally distributes to 0.83 v.u. per Bi–O bond; this translates to a bond length of 2.085 Å and a Raman stretching frequency of 493 cm^{-1}. Table II lists the estimated bond lengths and Raman stretching frequencies for the perfectly symmetric BiO_4, BiO_5, BiO_6, BiO_7, and BiO_8 structures.

The estimated Raman stretching frequencies for perfect BiO_x polyhedra (where x = 4, 5, 6, 7, 8) represent lowest-frequency values for a given oxygen coordination. For example, a perfect $Bi^{3+}O_6$ octahedron was

shown to have an expected Raman stretching frequency at 281 cm^{-1}. If this perfect octahedron were distorted in any way, then it would become polarized with respect to the distribution of valence electrons, resulting in a distribution of longer and shorter Bi–O bonds. In general, the Raman intensity of the shorter Bi–O bonds is expected to dominate because these are more covalent and therefore more polarizable. Consequently, as the distortion on the octahedral structure increases, the Bi–O stretching mode at 281 cm^{-1} shifts to higher wavenumber. The extent of this upward shift in frequency reflects the relative degree of distortion placed on the BiO_6 octahedron because as the structure is distorted, the distribution of Bi–O bond lengths becomes greater. Accordingly, for any given coordination type tabulated in Table II, the corresponding Raman stretching frequency represents a lower limit for that coordination. Distorted BiO_x polyhedra exhibit higher stretching frequencies than their perfect counterparts presented in Table II by an amount that is related to their degree of distortion.

The values tabulated in Table II for perfect BiO_x polyhedra may be compared with those distorted bismuth oxide structures listed in Table I. The sillenite structures (Bi : V = 60 : 1, $Bi_{12}GeO_{20}$, $Bi_{12}SiO_{20}$, $Bi_{12}TiO_{20}$, $Bi_{38}ZnO_{60}$), which are isomorphous with pure γ-Bi_2O_3, contain one general type of bismuth oxide polyhedron as well as a stabilizing metal cation impurity (V^{5+}, Ge^{4+}, Si^{4+}, Ti^{4+}, or Zn^{2+}) that occupies a nearly perfect tetrahedral site within the sillenite structure (*42*). The BiO_7 polyhedron in the sillenite structure has one short and four intermediate Bi–O bonds, which occupy five corners of an octahedron, and two very long Bi–O bonds of about 3.0–3.2 Å which occupy the sixth position of the octahedron and are separated by a "lone pair" of electrons. In fact, the BiO_7 polyhedron may be better represented as a BiO_5 polyhedron with one very short apical bond of 2.0–2.1 Å, two intermediate bonds of about 2.2 Å, and two longer bonds of about 2.6 Å. The corresponding Bi–O Raman stretching frequencies for these bonds are at about 527–538, 310–373, and 127–139 cm^{-1}. A comparison of these stretching frequencies to that of the perfect BiO_5 structure at 347 cm^{-1} reflects the distortion exhibited by the BiO_5 polyhedron in the sillenite structure.

The double perovskite structure of $BaBiO_3$ has alternating $Bi^{3+}O_6$ and $Bi^{5+}O_6$ octahedra with respective average Bi–O bond lengths of 2.28 and 2.12 Å. The $Bi^{3+}O_6$ unit in $BaBiO_3$ exhibits a Raman stretching band at 308 cm^{-1}, while the $Bi^{5+}O_6$ unit exhibits its Bi–O stretch at 563 cm^{-1}. These values may be compared with those estimated for the corresponding perfect octahedra, tabulated in Table II, at 281 cm^{-1} for $Bi^{3+}O_6$ and 493 cm^{-1} for $Bi^{5+}O_6$. The observed Raman stretching frequencies are higher than those predicted for the perfect BiO_6 structures—higher by 70 cm^{-1}, or 2.2σ, for $Bi^{5+}O_6$ and by 27 cm^{-1}, or 0.84σ, for $Bi^{3+}O_6$—reflecting the degree of distortion present in the $BaBiO_3$ structure. Clearly, the $Bi^{3+}O_6$ octahedron in $BaBiO_3$ is very regular while the $Bi^{5+}O_6$ octahedron is distorted.

2. Determining the molecular structures of the bismuth oxide polyhedra in the β- and δ-phases of Bi_2O_3. The crystal structure of β-Bi_2O_3 is tetragonal, space group $P42_1c$, with cell dimensions a = 7.7425 Å and c = 5.613 Å as determined as 643°C (*43*). The molecular structure of the bismuth oxide polyhedra in β-Bi_2O_3 were proposed to be BiO_6 octahedra with all bonds equivalent at 2.40 Å, although the reasoning was based on the erroneous space group $P4b_2$-D^7_{2d} (*14, 43*).

The δ-phase of Bi_2O_3 possesses a high degree of disorder that resembles the liquid state (*43*). The crystal structure was reported to be cubic (fluorite-related) and belong to the space group $Fm3m$ with a very

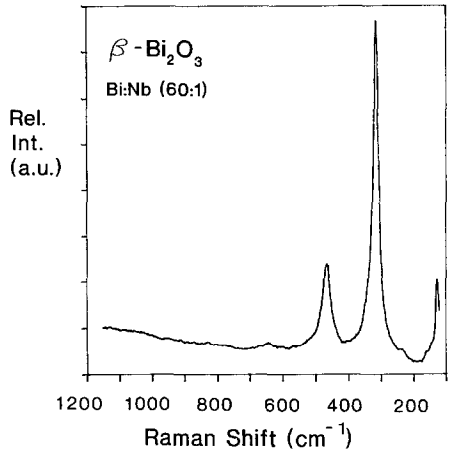

FIG. 3. The Raman spectrum of a niobia-stabilized β-Bi_2O_3 (Bi : Nb = 60 : 1).

large lattice parameter of at least a = 44.0 Å (*26*). It was postulated that the bismuth oxide polyhedra may be present as BiO_6, BiO_7, or BiO_8 units, depending on their proximity to the stabilizing cation (Nb^{5+} or Ta^{5+}).

The Raman spectra of the β- and δ-phases of Bi_2O_3 are presented in Fig. 3 and 4. The Raman spectrum of β-Bi_2O_3, shown in Fig. 3, exhibits three sharp bands at 462, 311, and 124 cm^{-1}. Initially, all three of these bands are assumed to be due to Bi–O stretches and are consequently expected to directly reflect bond lengths and strengths by Eqs. (3) and (4). Table III outlines the procedure for determining the bismuth oxide structure in β-Bi_2O_3; this procedure has previously been used to determine the molecular structures for several metal oxide systems (*20–25*). For β-Bi_2O_3, the three observed Bi–O stretches represent three unique Bi–O bond types present in its structure, and these are labeled A, B, and C. These three frequencies are converted to bond strengths, s (v.u.), and bond lengths, R (Å), by Eqs. (3) and (4). A QuickBASIC computer program was used to add every possible combination of bond strengths consistent with the formal oxidation state of the bismuth cation within a specified tolerance of 0.21 v.u.; according to the valence sum

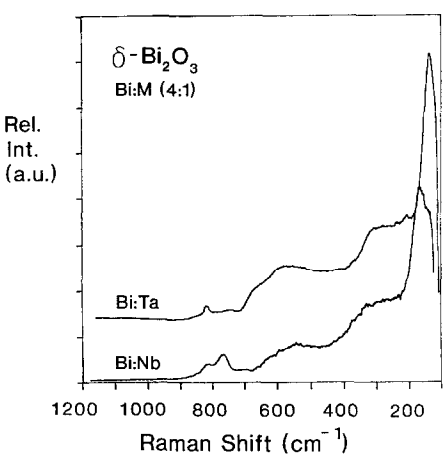

FIG. 4. The Raman spectra of niobia-stabilized δ-Bi_2O_3 (Bi : Nb = 4 : 1) and tantala-stabilized δ-Bi_2O_3 (Bi : Ta = 4 : 1).

TABLE III

β-Bi_2O_3 STRUCTURE DETERMINATION BY RAMAN SPECTROSCOPY

Observed Raman bands	Bi–O stretches: 462,311,124 cm^{-1}		
Bi–O bond types	ν	s (v.u.)	R (Å)
A	462	0.782	2.111
B	311	0.546	2.269
C	124	0.258	2.635

Possible structures	Coordination	A	B	C	Valence (v.u.)
(a)	4	4	0	0	3.162
(b)	4	3	1	0	2.926
(c)	5	3	1	1	3.167
(d)	5	3	0	2	2.880
(e)	5	2	2	1	2.931
(f)	5	1	4	0	2.982
(g)	6	3	0	3	3.121
(h)	6	2	2	2	3.172
(i)	6	2	1	3	2.885
(j)	6	1	3	2	2.936
(k)	6	0	5	1	2.987

Best structure (ej)		
	1 × A	1 × 2.11(3) Å
	2 × AB	2 × 2.19(11) Å
	1 × B	1 × 2.27(3) Å
	2 × C	2 × 2.64(3) Å

TABLE IV

δ-Bi_2O_3 STRUCTURE DETERMINATION BY RAMAN SPECTROSCOPY

Observed Raman bands	Bi–O stretches: 550,320 cm^{-1}			
Bi–O bond types	ν	s (v.u.)		R (Å)
A	550	0.924		2.042
B	320	0.560		2.257
Possible structures	Coordination	A	B	Valence (v.u.)
(a)	3	3	0	2.824
(b)	4	2	2	3.002
(c)	5	1	4	3.180
(d)	5	0	5	2.815
Best structure	1 × A	1 × 2.04(3) Å		
(c)	4 × B	4 × 2.26(3) Å		

rule (*30, 31*), the sum of the individual bond valences at a metal cation site equals its formal oxidation state. Table III shows that 11 structures, (a) through (k), are possible from the available bond strengths for β-Bi_2O_3. After maximizing the number of Raman frequencies used and choosing the most consistent valence, two possible structures result, (e) and (j), from which a hybrid structure is formed and represents the "best" possible structure from the Raman data. As shown at the bottom of Table III, the best structure for the bismuth oxide species in β-Bi_2O_3 consists of a BiO_6 octahedron with bond lengths 1 × 2.11(3), 2 × 2.19(11), 1 × 2.27(3), and 2 × 2.64(3) Å.

The procedure described above for β-Bi_2O_3 is used to determine the average structure of the BiO_x polyhedron present in the impurity-stabilized δ-Bi_2O_3. The Raman spectrum of δ-Bi_2O_3, shown in Fig. 4, shows two broad bands at 550 and 320 cm^{-1} assigned to Bi–O stretches, and sharp bands below 200 cm^{-1} assigned to lattice vibrations (external modes are characteristically sharper than internal modes). Table IV shows that four structures are possible from the calculated bond strengths, but only structures (b) and (c) use both Raman frequencies. The $Bi^{3+}O_4$ tetrahedron depicted by structure (b), however, is not consistent with the known BiO_4 reference structures in Table I because of its geometric asymmetry with two very short bonds of 2.04 Å and two longer bonds of 2.26 Å. The only tetrahedron listed in Table I as a reference structure has a bismuth cation valence of 5.0 v.u., is extremely symmetric, and exhibits a sharp Raman stretching frequency at 827 cm^{-1}. A $Bi^{3+}O_4$ tetrahedron is unlikely because the Bi^{3+} cation is an asymmetric ion containing a lone $6s^2$ pair of electrons and completes its coordination polyhedron with five other atoms to form an octrahedron (*36*). Furthermore, according to Table I, a Raman stretching frequency at 550 cm^{-1} can best be fit to a distorted, monooxo-BiO_5 structure, for example, as found in the sillenite phases. This description matches that of the BiO_5 structure labeled as (c) in Table IV. Therefore, structure (c) is regarded as the best structure and consists of a BiO_5 polyhedron with one short bond of 2.04(3) Å (presumably positioned opposite the $6s^2$ lone pair of electrons) and four intermediate bonds of 2.23(3) Å.

In addition, the Raman spectrum of δ-Bi_2O_3, in Fig. 4, shows a small but well-defined peak at 821 cm^{-1}. This feature has been observed before in the sillenite structure of composition $Bi_{25+x}V_{1-x}O_{40}$, where x Bi^{5+} cations are expected to occupy the tetrahedral sites in vanadium-deficient $Bi_{25}VO_{40}$ (*34*). For the Bi–V–O system, the combined interpretation of the Raman and ^{51}V solid state NMR data provided strong evidence for the presence of $Bi^{5+}O_4$ tetrahedra. By analogy, the small peak in the Raman spectrum of δ-Bi_2O_3 is also assigned to a $Bi^{5+}O_4$ tetrahedron with estimated Bi–O bond lengths of about 1.92(2) Å (from Eq. (2)).

The molecular structures of the bismuth oxide species proposed for the β- and δ-phases of Bi_2O_3 may be compared with previously postulated models. The β-phase

of Bi_2O_3 was proposed to contain BiO_6 octahedra with all Bi–O bonds equivalent at 2.40 Å (*14, 43*). This model is similar to that derived in the present study, except the BiO_6 octahedron is presently found to have bond lengths ranging from 2.11 to 2.64 Å, similar to those present in α-Bi_2O_3 (see Table I). The δ-phase of Bi_2O_3 was postulated to have BiO_6, BiO_7, or BiO_8 units depending on their proximity to the stabilizing cation (Nb^{5+} or Ta^{5+}) (*43*). In the present study, however, δ-Bi_2O_3 is found to have BiO_5 units similar to those in sillenite, with one short apical Bi–O bond and four intermediate Bi–O bonds. Another similarity between the structure of the δ-phase and sillenite phase (γ-phase) is that both contain $Bi^{5+}O_4$ tetrahedra, with the tetrahedron in δ-Bi_2O_3 (ν = 821 cm^{-1}) being slightly more symmetric than that in the sillenite phases (ν = 827 cm^{-1}). Thus, the molecular structure of the bismuth oxide polyhedron in β-Bi_2O_3 is similar to that found in α-Bi_2O_3, while those in δ-Bi_2O_3 are more closely related to the sillenite or γ-Bi_2O_3 structure.

VI. Conclusions

A method was presented for determining the molecular structures of bismuth oxide species from an analysis of their Raman spectra. The method relies on empirical expressions relating bismuth–oxygen bond lengths, Raman stretching frequencies, and Pauling bond strengths (in valence units). The utility of the method was illustrated by estimating the Bi–O bond lengths and Raman stretching frequencies for ideally symmetric bismuth oxide structures BiO_4, BiO_5, BiO_6, BiO_7, and BiO_8. The method was further used to determine the structure of the bismuth oxide species in the β- and δ-phases of Bi_2O_3: β-Bi_2O_3 consists of a $Bi^{3+}O_6$ octahedron with bond lengths 1 × 2.11(3), 2 × 2.19(11), 1 × 2.27(3), and 2 × 2.64(3) Å; δ-Bi_2O_3 consists of a regular $Bi^{5+}O_4$ tetrahedron as a minor structure with all bond lengths of 1.92(3) Å, and a $Bi^{3+}O_5$ polyhedron as the major structure with bond lengths 1 × 2.04(3) and 4*x* 2.26(3) Å. The structure of the bismuth oxide species in β-Bi_2O_3 was found to be similar to that found in α-Bi_2O_3, while the structure of δ-Bi_2O_3 is similar to that of the sillenite or γ-Bi_2O_3 phases. The method developed in the present study for determining the bond lengths and coordinations of BiO_x polyhedra provides much insight into the molecular structures of bismuth oxide phases and holds promise as a highly effective tool for which to study systems that cannot be routinely examined by diffraction methods.

Acknowledgments

The authors are indebeted to D. A. Jefferson, D. A. Buttrey, W. Zhou, and J. M. Thomas for supplying the impurity-stabilized β-, δ-, and γ-phases of Bi_2O_3. Financial support from the Texaco Philanthropic Foundation and the Sherman Fairchild Foundation is acknowledged by F.D.H.

References

1. L. G. Sillen, *Ark. Kemi Mineral. Geol. A.* **12,** 1 (1937).
2. H. A. Harwig and A. G. Gerards, *J. Solid State Chem.* **26,** 265 (1978).
3. D. A. Jefferson, J. M. Thomas, M. K. Uppal, and R. K. Grasselli, *J. Chem. Soc. Chem. Commun.*, 594 (1983).
4. J. M. Thomas, D. A. Jefferson, and G. R. Millward, *JOEL News E* **23,** 7 (1985).
5. W. Zhou, D. A. Jefferson, M. Alario-Franco, and J. M. Thomas, *J. Phys. Chem.* **91,** 512 (1987).
6. A. A. Agasiev, V. E. Bagiev, A. M. Mamedov, and Y. Y. Guseinov, *Phys. Status Solid; B* **149,** K191 (1988).
7. A. Harriman, J. M. Thomas, Z. Wuzong, and D. A. Jefferson, *J. Solid State Chem.* **72,** 126 (1988).
8. A. V. Chadwick, W. Zhou, and J. M. Thomas, *Angew. Chem.* **101,** 69 (1989); *Angew. Chem. Int. Ed. Engl.* **28,** 75 (1989).
9. P. V. Lenzo, E. G. Spencer, and A. A. Ballman, *Appl. Opt.* **5,** 1688 (1966).
10. G. F. Moore, P.V. Lenzo, E. G. Spencer, and A. A. Ballman, *J. Appl. Phys.* **40,** 2361 (1969).

11. A. FELDMAN, W. S. BROWER, JR., AND D. HOROWITZ, *Appl. Phys. Lett.* **16,** 201 (1970).
12. W. C. SCHUMB AND E. S. RITTNER, *J. Am. Chem. Soc.* **65,** 1055 (1943).
13. G. GATTOW AND H. SCHRODER, *Z. Anorg. Allg. Chem.* **318,** 176 (1962).
14. G. GATTOW AND H. SCHUTZE, *Z. Anorg. Allg. Chem.* **328,** 44 (1964).
15. E. M. LEVIN AND R. S. ROTH, *J. Res. Natl. Bur. Stand. A* **68,** 189 (1964).
16. C. N. R. RAO, G. V. SUBBA RAO, AND S. RAMDAS, *J. Phys. Chem.* **73,** 672 (1969).
17. K. NAKAMOTO, "Infrared and Raman Spectra of Inorganic and Coordination Compounds," 3rd ed., Wiley, New York (1978).
18. L. DIXIT, D. L. GERRARD, AND H. J. BOWLEY, *Appl. Spectrosc. Rev.* **22,** 189 (1986).
19. I. E. WACHS, F. D. HARDCASTLE, AND S. S. CHAN, *Spectroscopy* **1,** 30 (1986).
20. F. D. HARDCASTLE, "Molecular Structures of Bulk and Surface Metal Oxides by Raman Spectroscopy: The Diatomic Approximation," Dissertation, Lehigh University, Bethlehem, PA; University Microfilms International, Ann Arbor, MI.
21. F. D. HARDCASTLE AND I. E. WACHS, *J. Raman Spectrosc.* **21,** 683 (1990).
22. F. D. HARDCASTLE AND I. E. WACHS, *J. Phys. Chem.*, **95,** 5031 (1991).
23. F. D. HARDCASTLE AND I. E. WACHS, *Solid State Ionics*, **45,** 201 (1991).
24. F. D. HARDCASTLE AND I. E. WACHS, submitted for publication.
25. F. D. HARDCASTLE AND C. H. F. PEDEN, submitted for publication.
26. W. ZHOU, D. A. JEFFERSON, AND J. M. THOMAS, *Proc. R. Soc. London A* **406,** 173 (1986).
27. W. ZHOU, *J. Solid State Chem.* **76,** 290 (1988).
28. W. ZHOU, D. A. JEFFERSON, AND J. M. THOMAS, *J. Solid State Chem.* **70,** 129 (1987).
29. W. G. FATELEY, F. R. DOLLISH, N. T. MCDEVITT, AND F. F. BENTLEY, "Infrared and Raman Selection Rules for Molecular and Lattice Vibrations: The Correlation Method," Wiley–Interscience, New York (1972).
30. I. D. BROWN, *Chem. Soc. Rev.* **7,** 359 (1978).
31. I. D. BROWN AND K. K. WU, *Acta Crystallogr. B* **32,** 1957 (1976).
32. K. P. HUBER AND G. HERZBERG, "Molecular Spectra and Molecular Structure: Constants of Diatomic Molecules," Van Nostrand–Reinhold, New York (1979).
33. D. E. COX AND A. W. SLEIGHT, *Solid State Commun.* **19,** 969 (1976).
34. F. D. HARDCASTLE, I. E. WACHS, H. ECKERT, AND D. A. JEFFERSON, *J. Solid State Chem.* **90,** 194 (1991).
35. R. J. BETSCH AND W. B. WHITE, *Spectrochim. Acta* **34,** 505 (1978).
36. D. C. CRAIG AND N. C. STEPHENSON, *J. Solid State Chem.* **15,** 1 (1975).
37. G. M. SAFRONOV, V. N. BATOG, T. V. STEPANYUK, AND P. M. FEDOROV, *Russ. J. Inorg. Chem.* **16,** 460 (1971).
38. YU. F. KARGIN, A. A. MAR'IN, AND V. M. SKORIKOV, *Izv. Akad., Nauk SSSR Neorg. Mater.* **18,** 1375 (1982).
39. F. L. GALEENER, *Solid State Commun.* **44,** 1037 (1982).
40. F. L. GALEENER, *in* "The Structure of Non-Crystalline Materials. Proceedings of the 2nd International Conference" (P. H. Gaskell, J. M. Parker, and E. A. Davis, Eds.), pp. 337–359, International Publications Service, Taylor & Francis, London (1983).
41. E. BRIGHT WILSON, JR., J. C. DECIUS, AND P. C. CROSS, "Molecular Vibrations: The Theory of Infrared and Raman Vibrational Spectra," Dover, New York (1980).
42. H. S. HOROWITZ, A. J. JACOBSON, J. M. NEWSAM, J. T. LEWANDOWSKI, AND M. E. LEONOWICZ, *Solid State Ionics* **32/33,** 678 (1989).
43. H. A. HARWIG, *Z. Anorg. Allg. Chem.* **444,** 151 (1978).
44. D. C. N. SWINDELLS AND J. L. GONZALEZ, *Acta Crystallogr. B* **44,** 12 (1988).